DOI: 10.1016/S1872-5805(22)60608-5

Hydrothermal synthesis of carbon nanodots from waste wine cork and their use in biocompatible fluorescence imaging

Quang Ngo Khoa[1,*], Hieu Nguyen Ngoc[2,3], Bao Vo Van Quoc[4], Phuoc Vo Thi[1], Ngoc Le Xuan Diem[1], Doc Luong Quang[1], Tri Nguyen Minh[1], Son Le Vu Truong[5], Son Le Van Thanh[5], Ha Che Thi Cam[1]

(1. *University of Sciences*, *Hue University*, *77 Nguyen Hue*, *Hue*, *Vietnam*;

2. *Faculty of Environmental and Natural Sciences*, *Duy Tan University*, *Da Nang*, 550000, *Vietnam*;

3. *Institute for Research and Training in Medicine*, *Biology and Pharmacy*, *Duy Tan University*, *Da Nang*, 550000, *Vietnam*;

4. *University of Agriculture and Forestry*, *Hue University*, 102 *Phung Hung*, *Hue*, *Vietnam*;

5. *University of Science and Education*, *The University of Da Nang*, 459 *Ton Duc Thang*, *Lien Chieu*, *Da Nang*, *Vietnam*)

Abstract: A low-cost and simple method is reported for the synthesis of carbon nanodots (CDs) from waste wine cork using hydrothermal treatment. The structural and optical properties of the CDs were characterized by TEM, FTIR, Raman, UV-Vis absorption, and photoluminescence (PL) spectroscopy. Results indicate that the CDs have an average diameter of ~ 6.2 ± 2.7 nm and their excitation-dependent PL is related to the functional groups on their surface. The CDs have a quantum yield of 1.54%, estimated using quinine sulfate as a reference. They have been successfully applied in the bioimaging of mesenchymal stem cells (MSCs). After treatment with the CDs, the MSCs fluoresce green, yellow and red colors under the excitation wavelengths in the ranges 320-380 nm, 450-490 nm, and 515-560 nm, respectively, demonstrating their potential use in the field of fluorescence imaging.

Key words: Carbon nanodots; Hydrothermal synthesis; Fluorescence; Fluorescent image; Waste wine cork

1 Introduction

Recent nanostructure fabrication methods have allowed researchers to synthesize materials with revolutionary potential applications[1–4]. There are multiple ways to prepare materials at the nanometer scale. They can be divided into two routes, the bottom-up and top-down methods[5–12]. The development of fabrication techniques offers many advantages. At the same time, it also prompts scientists to search for novel nanoscale materials, overcoming the limitations of conventional ones. In terms of carbon nanomaterials, the discovery of carbon nanodots (CDs) should be a case. Although CDs were accidentally discovered by Xu et al. when they purified single-walled carbon nanotubes. CDs constitute fluorescent active groups, which are related to many intriguing optical features[13].

CDs have been defined as carbon nanoparticles with sizes below 10 nm[14,15]. CDs are specifically novel kinds of nanoparticles possessing intrinsic optical properties, which have high biocompatibility, excellent photostability, and the excitation-dependent photoluminescence[16–21]. Hence, in recent years, numerous research groups have reported a broad range of applications of CDs, including biological labeling, drug delivery, chemical and biosensors, bioimaging, electrocatalysis, etc[22–25]. For biomedical applications, CDs are considered as a potential solution of future-expected fluorescent nanomaterials since they take advantage of traditional semiconductor quantum dots together with their unique characteristic of likely lower cytotoxicity[20, 26, 27].

For synthesizing CDs, the chemical oxidation method is convenient and fast for large-scale production. However, treatment usually employs strong acid to provide an oxidative environment[4,18]. Thus, this method leads to disadvantages related to environmental concerns. A green and simple preparation method is highly desired to overcome the limitation of complex synthesis routes, the involvement of toxic, or expensive reagents.

In recent years, the hydrothermal method is considered as a cost-effective chemical route for the con-

Received date: 2021-06-15; **Revised date:** 2021-08-23

Corresponding author: Quang Ngo Khoa. E-mail: nkquang@hueuni.edu.vn

version of carbon precursors[28–32]. The treatment utilizes aqueous media at elevated temperatures and pressures for reactions[2]. At such a state, water becomes a reactive substance, allowing chemical reactions such as cellulose hydrolysis and biomass refining in general without the addition of strong acids[33]. Swagatika Sahu et al. proposed a plausible mechanism, in which orange juice went through dehydration, condensation, polymerisation, and aromatisation under hydrothermal treatment. When the concentration of aromatic clusters reached a critical supersaturation point, a burst nucleation occurred and CDs were formed[18]. In another pioneering work, a detailed investigation of the hydrothermal transformation of glucose, carbohydrates, cellulose, and biomass (rye straw) was carried out by Niki Baccile and co-workers[33]. According to the literature, the starting material underwent thermochemical degradation during hydrothermal synthesis to yield carbon nanoparticles[4,18,33].

From the above-mentioned works, we could perceive that carbonaceous materials result from widely available precursors. Not only the chemical reagents but also the natural sources can be used as the precursors for this method. Previous works have addressed that green biomass precursors could provide an ideal strategy to prepare green fluorescent CDs, especially waste materials[34–38]. Herein, the preparation of CDs from waste wine cork (made by cork oak) by hydrothermal treatment is described. The rationale for the selection of wine cork is considered since the polysaccharide content of cork is up to 20.9% in the chemical composition[39]. As previously published, many polysaccharide-rich materials are successfully employed to synthesize CDs[40]. The characterization techniques of the obtained CDs include TEM, FTIR, UV-Vis absorption, and photoluminescence (PL) spectroscopy. Furthermore, we attempt to probe biocompatibility by incubating mesenchymal stem cells (MSCs) from human umbilical cord (UC) with the obtained CDs. The purpose of this work is to provide information in regulating the microstructures of the CDs synthesized from wine cork for bioimaging applications.

2 Experimental

2.1 Materials

DMEM/F12 medium, fetal bovine serum (FBS), and proxacin were purchased from Miltenyi Biotec, Germany.

2.2 Synthesis of CDs

Waste wine cork of Vang Đàlạt® red wine from Ladofoods Co., Ltd. (Ladofoods, Lam Dong, Vietnam) was used as the raw material. The wine cork (5.0 g) was first washed with water to remove surface dirt and dried in an oven before it was cut into small pieces. Then, It was mixed with 80 mL of distilled water and transferred into a 100 mL Teflon-lined autoclave. The resulting mixture was heated at 220 °C for 4 h in the autoclave. After cooled down to room temperature naturally, the brown-black carbonized solution was roughly purified through a 0.22 μm microporous membrane. Subsequently, the solution was centrifuged at 14 000 r min^{-1} for 15 min to remove the large particles. Finally, the obtained CDs were stored at 4 °C for further use. It was estimated that 0.51 mg mL^{-1}, implying the yield was approximately 0.20%.

2.3 In vitro cell imaging with CDs

The commercial mesenchymal stem cells (MSCs) of the human umbilical cord (UC) were purchased from Hue Central Hospital (Hue, Vietnam). Then, the MSCs (1×10^3 cells/cm^2) were cultured on a 6-well plate, in the growth medium of DMEM/F12 supplemented with 10% FBS and 1% proxacin. The cells were incubated in a humidified atmosphere containing 5% CO_2 and 95% air at 37 °C for 5-6 weeks. Twice a week, the medium was substituted, and morphology was examined under inverted optical microscopy. When the cells were approximately 60% confluent, the CD solution with a concentration of 0.25× (1× = 0.51 mg/mL) was deliberately added to the cell dishes. After incubated further for 2 h, the cells were washed with PBS three times to remove the free CDs attached on the outer surface of the cell membrane. Cell fluorescent images were detected with the excita-

tion wavelengths set in a range 320-380, 450-490 and 515-560 nm.

2.4 Cytotoxicity test on MSCs

Followed by the incubation of MSCs, CD solution at various concentrations was added to the culture medium. Images of the MSCs at each test concentration were captured (by Olympus CKX31 microscope) in three different fields to estimate error bars. MSC numbers were assessed by using the ImageJ software. Cell viability in the control sample at 0 h was considered to be 100% and the cell viability percentage with different doses of CDs (0.1×, 0.25×, 0.5×, 0.75×, 1× = 0.51 mg mL^{-1}) at 0 h were compared with this value. For each value of CD concentration, the cell viability over incubation time (2, 4 and 6 h) was determined by the following Equation (1):

$$Cell\ viability\ (\%) = \frac{Cells_{(S)}}{Cells_{(C)}} \times 100 \qquad (1)$$

Where, $Cells_{(S)}$ and $Cells_{(C)}$ are the total number of viable cells at each incubation time and the total number of viable cells at 0 h, respectively.

2.5 Quantum yield (QY) measurements

CDs with a QY of 1.54% was calculated using quinine sulfate as a reference. The quantum yield of the CDs was determined by a comparative method in which quinine sulfate (literature QY = 0.54) was used as a reference. Four concentrations of CD solutions were made by dispersing CDs in water (refractive index (n) of 1.33) while quinine sulfate was dissolved in 0.1 mol L^{-1} H_2SO_4 (n = 1.33). All the absorbance values of the solutions at the excitation wavelength were less than 0.1. Photoluminescence (PL) emission spectra of all the sample solutions were recorded at an excitation wavelength of 340 nm. The integrated fluorescence intensity was the area under the PL curve in the wavelength range from 360 to 700 nm. The QY was calculated using the slope of the line determined from the plot of the absorbance against the integrated fluorescence intensities as in the Equation (2):

$$QY = QY_r\left(\frac{m}{m_r}\right).\left(\frac{n^2}{n_r^2}\right) \qquad (2)$$

Where, m is the slope, n is the refractive index of solvent, and the subscript "r" refers to the referenced sample.

2.6 Instrument

XRD pattern of the obtained CDs was obtained on a D8 Advance (Bruker, Germany) in the range from 10° to 60°. The size and morphology of the CDs were observed on a transmission electron microscope (TEM) JEOL JEM–1010 (JEOL, Japan) with an accelerating voltage of 80 kV. For optical properties, UV–vis absorption spectra of the samples were recorded on a GENESYS 10S UV-Vis (Thermo Scientific, American). Fluorescence spectroscopy was carried out on a FS5 spectrofluorometer (Edinburgh Instrument, UK). Fourier-transform infrared (FTIR) spectroscopy was carried out on a FTIR Affinity-1S (Shimadzu, Japan). The Raman spectra of obtained samples were recorded with a Horiba XploRA PLUS (Horiba, Japan) using excitation at 785 nm. Fluorescence imaging was performed with an optical microscope Leica DM2500 (Leica, Germany) and the specimens were excited by a halogen lamp in a range 320-380, 450-490 and 515-560 nm.

3 Results and discussion

From the photo presented in Fig. 1a, it can be seen that the aqueous solution containing CDs shows the visible green color under laser irradiation of 405 nm wavelength. In comparison to that under room light, this evidence confirms the formation of fluorescent product that can be seen with the naked eyes. As can be seen from Fig. 1b, the TEM image indeed indicates that the obtained particles have an uniform dispersion without obvious aggregation. Specifically, the size histogram of particles presented in Fig. 1c indicates that the average diameter of CDs ~ 6.2 ± 2.7 nm is comparable to the previous report[36, 37].

The phase of the obtained CDs was clarified by X-XRD pattern and Raman spectrum. The XRD pattern shown in Fig. 2a illustrates a broad peak at ≈22° and this should be consistent with the (002) lattice spacing, indicating the highly amorphous characteristic of carbon-based materials[18]. Indeed, annealing temperatures were modified to probe the product re-

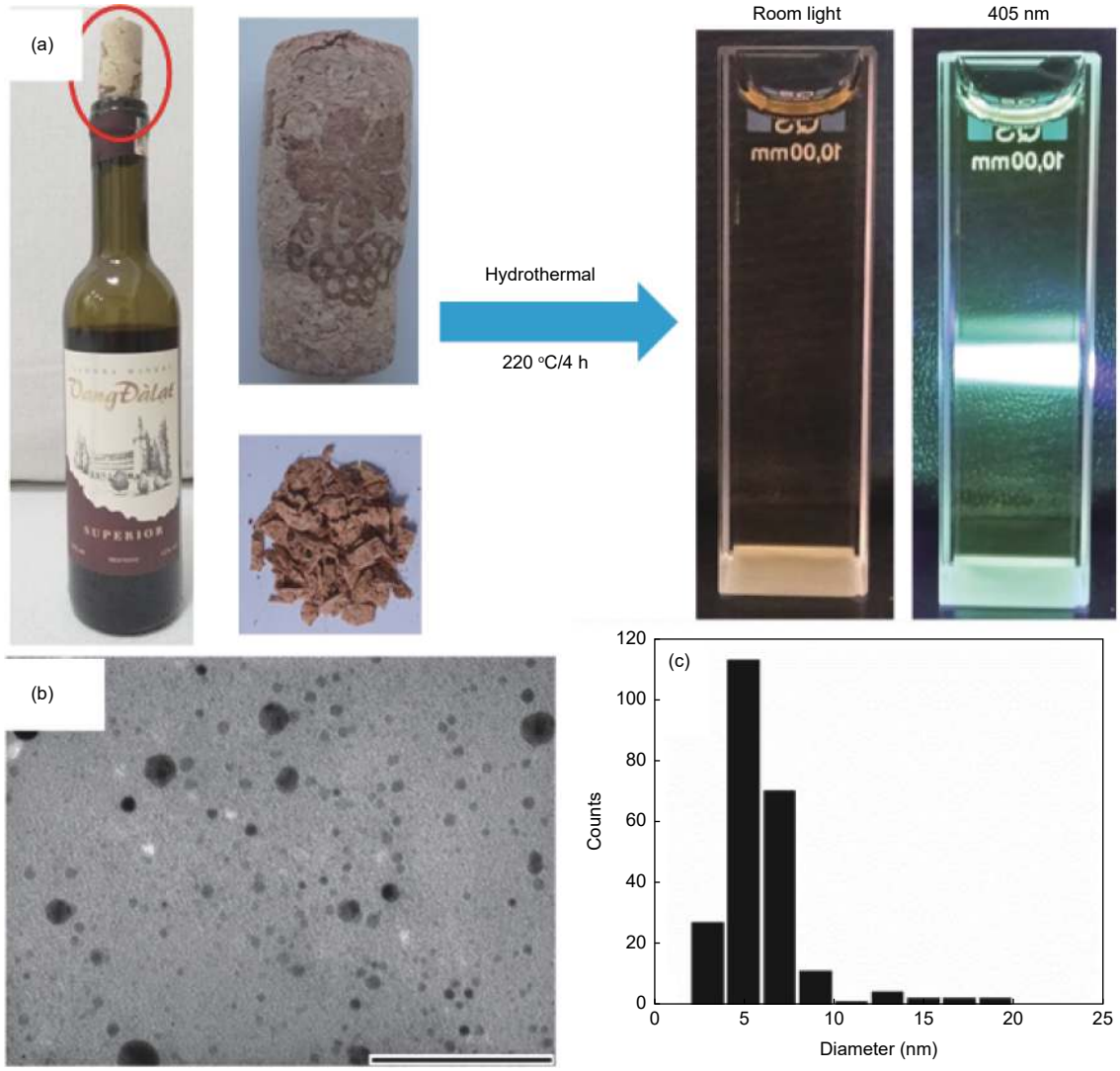

Fig. 1 (a) Illustration of the CD synthesis process from wine cork and photos of the CD solution under room light and 405 nm laser light, (b) TEM image of the obtained CDs with the scale bar of 100 nm and (c) the corresponding size distribution.

sponse. The Raman signal of the sample used in this study exhibits the stronger intensity of *D*-band (sp^3 hybridized carbon atoms) compared with that of *G*-band (vibrations of sp^2 hybridized carbon atoms) with an intense peak and a shoulder at around 1 370 and 1 570 cm^{-1}, respectively. The result obtained in Fig. 2b further proves the amorphous nature of the wine cork-derived CDs[41,42].

The optical properties of CDs were investigated by UV-vis absorption and emission spectra. The UV-vis absorption spectrum shown in Fig. 3a indicates 2 peaks at around 217 and 280 nm and similar UV–vis spectrum was reported in previous publications, which are attributed to π–π^* transition of the C=C and n–π^* transition of the C=O bonds, respectively[40]. To further clarify optical behavior, fluorescence spectra of the obtained CDs were examined. In early studies, CDs exhibite the dependence of the emission on the excitation wavelength[37, 41]. Similarly, in our case, there is an obvious shift as the excitation wavelength varies, as shown in Fig. 3b. Particularly, the corresponding contour shown in Fig. 3c reveals a fluorescence band with the peak emission intensity at a wavelength of ~435 nm. For CDs, the PL mechanism is the most important in terms of investigation. The emission peak position is usually related to the excitation wavelength. Although the origin of fluorescence in CDs is not yet entirely understood, the wide size distribution of CDs and surface states generally result in this behavior[43–45].

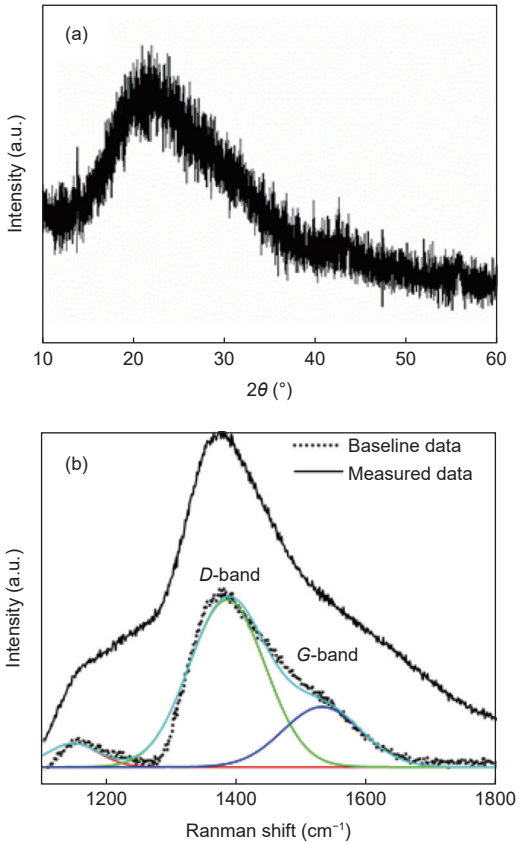

Fig. 2　(a) XRD pattern and (b) Raman spectrum of the obtained CDs.

Subsequently, the chemical structure and composition of functional groups onto the surfaces of the CDs were investigated by FITR. The result is shown in Fig. 4. The characteristic absorption bands indeed reflect the functional groups, including the O—H stretching vibration at 3 421 cm^{-1}, the C—H stretching vibration at 2 927 and 2 856 cm^{-1}, the N—H bending vibration at 1 651 cm^{-1}, and the C=O stretching vibration at 1 631 cm^{-1}[37,46–48]. In addition, peaks at 1 402 and 1 060 cm^{-1} are resulted from the C—O—C asymmetric and symmetric stretching vibration[49]. According to the above-mentioned assignments, the FTIR spectrum reveals the functional groups on the surface of CDs after the thermal reaction, which are very important in bioconjugation and for further bioimaging.

Fig. 5a indicates the cytotoxicity of CDs evaluated after the MSCs are treated with different doses of CDs. The CDs at various concentrations are added to the culture medium when the cells are approximately 60% confluent. Therefore, cells continue to proliferate if the CDs do not affect cell division. The values after incubation of the control sample (no treatment of CDs) for 2, 4 and 6 h with a concentration of 0.1× are all higher than 100%. As shown in Fig. 5a, the obtained-CDs do not impose any significant toxicity to cells at concentrations up to 0.25× after incubation for 6 h. The results also indicate that the cell viability at the concentrations of 0.5×, 0.75× and 1× dramatically decreases with increasing the exposure time, indicating their less efficiency for the growth of the cells. In the bright-field optical image (Fig. 5b), the cells show no substantial change in shape after treatment with the CDs. As shown in Fig. 5c, 5d and 5e, MSCs exhibit fluorescence including green, yellow and red colors under violet (320-380 nm), blue (450-490 nm), and green (515-560 nm) light excitation, respectively. Meanwhile, the control sample without treatment of the CDs shows no photoluminescence at the same exposure conditions (data not shown). The results are consistent with the previous publications[50, 51]. The excitation-dependent PL makes it possible for multiple color emission in cells imaged by using CDs only.

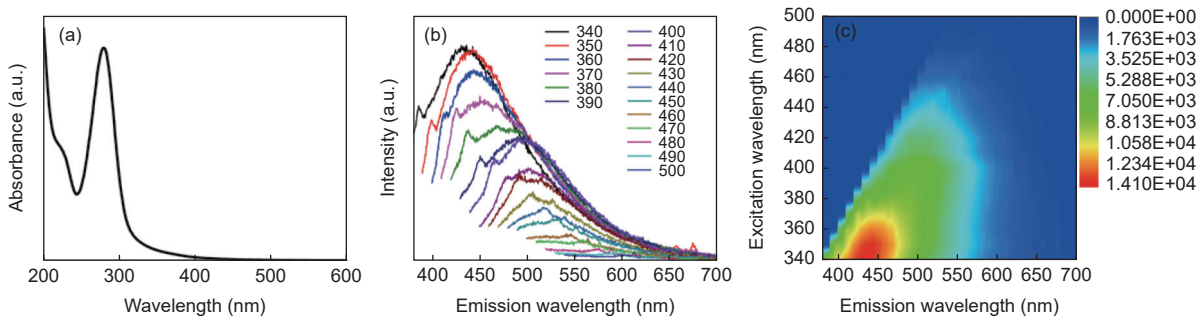

Fig. 3　(a) UV–Vis absorption spectrum of CDs, (b) PL spectra of the obtained CDs under different excitation wavelengths from 340 to 500 nm (in 10 nm increment starting from 340 nm) and (c) the corresponding contour plot.

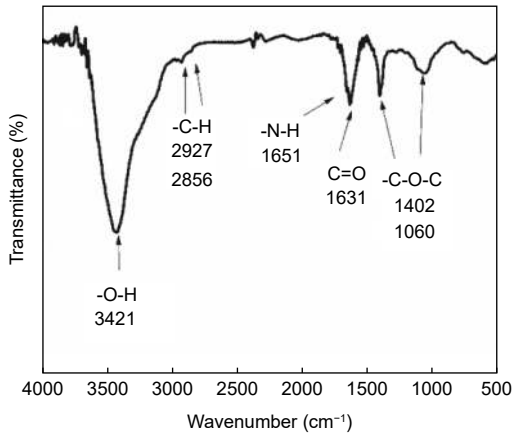

Fig. 4 FTIR spectrum reflecting the functional groups on the surface of CDs.

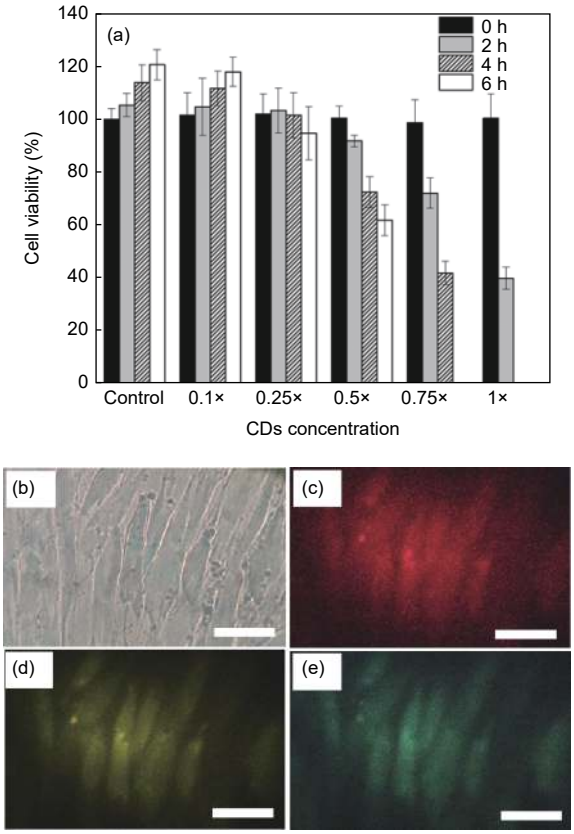

Fig. 5 Cytotoxicity and cell imaging. (a) Cells treated with CDs having concentrations of 0, 0.1×, 0.25×, 0.5×, 0.75× and 1× for 0 h, 2 h, 4 h and 6 h, respectively (1× = 0.51 mg mL^{-1}). MSCs incubated with the CDs under, (b) transmission light, (c) green (515-560 nm), (d) blue (450-490 nm) and (e) violet (320-380 nm) light excitation. Scale bar is 50 μm.

4 Conclusion

Multi colorful fluorescent CDs were successfully synthesized from waste wine cork by hydrothermal treatment. The wine cork-derived CDs exhibit bright fluorescence under different excitation wavelengths. Furthermore, the CDs have been successfully applied in MSC imaging. The results show that the CDs could be employed as a solution for bioimaging due to their bright and multicolor luminescence. The achievements suggest further applications in the field of both photoluminescent and fluorescent imaging.

Acknowledgment

We gratefully acknowledge the financial support of the Vietnam Ministry of Education and Training with Grant No. B2021-DHH-05. The author also acknowledges feedback from anonymous reviewers, which helped improve the final version of the paper.

References

[1] Li H, Kang Z, Liu Y, et al. Carbon nanodots: Synthesis, properties and applications[J]. J Mater Chem, 2012, 22: 24230-24253.

[2] Wang Y, Hu A. Carbon quantum dots: Synthesis, properties and applications[J]. J Mater Chem C, 2014, 2: 6921-6939.

[3] Liu M L, Chen B B, Li C M, et al. Carbon dots: Synthesis, formation mechanism, fluorescence origin and sensing applications[J]. Green Chem, 2019, 21: 449-471.

[4] Meng W, Bai X, Wang B, et al. Biomass-derived carbon dots and their applications[J]. Energy Environ Mater, 2019, 2: 172-192.

[5] Sun Y-P, Zhou B, Lin Y, et al. Quantum-sized carbon dots for bright and colourful Photoluminescence[J]. J Am Chem Soc, 2006, 128: 7756-7757.

[6] Hu S L, Niu K Y, Sun J, et al. One-step synthesis of fluorescent carbon nanoparticles by laser irradiation[J]. J Mater Chem, 2009, 19: 484-488.

[7] Zhou J, Booker C, Li R, et al. An electrochemical avenue to blue luminescent nanocrystals from multiwalled carbon nanotubes (MWCNTs)[J]. J Am Chem Soc, 2007, 129: 744-745.

[8] Liu H, Ye T, Mao C. Fluorescent carbon nanoparticles derived from candle soot[J]. Angew Chem Int Ed, 2007, 46: 6473-6475.

[9] Zhu H, Wang X, Li Y, et al. Microwave synthesis of fluorescent carbon nanoparticles with electrochemiluminescence properties[J]. Chem Commun, 2009, 34: 5118-5120.

[10] Qu S, Wang X, Lu Q, et al. A biocompatible fluorescent ink based on water-soluble luminescent carbon nanodots[J]. Angew Chem Int Ed, 2012, 51: 12215-12218.

[11] Liu R, Wu D, Liu S, et al. An aqueous route to multicolor photoluminescent carbon dots using silica spheres as carriers[J]. Angew Chem Int Ed, 2009, 121: 4668-4671.

[12] Sun X, Brückner C, Lei Y. One-pot and ultrafast synthesis of nitrogen and phosphorus co-doped carbon dots possessing bright dual wavelength fluorescence emission[J]. Nanoscale, 2015, 7:

17278-17282.

[13] Xu X Y, Ray R, Gu Y L, et al. Electrophoretic analysis and purification of fluorescent single-walled carbon nanotube fragments[J]. J Am Chem Soc, 2004, 126(40): 12736-12737.

[14] Nevar A, Tarasenka N, Nedelko M, et al. Carbon nanodots with tunable luminescence properties synthesized by electrical discharge in octane[J]. Carbon Lett, 2021, 31: 39-46.

[15] Yang N, Jiang X, Pang D W. Carbon Nanoparticles and Nanostructures. Switzerland: Springer, 2016: 243-249.

[16] Zhou J, Sheng Z, Han H, et al. Facile synthesis of fluorescent carbon dots using watermelon peel as a carbon source[J]. Mater Lett, 2012, 66(1): 222-224.

[17] Lim S Y, Shen W, Gao Z. Carbon quantum dots and their applications[J]. Chem Soc Rev, 2015, 44(1): 362-381.

[18] Sahu S, Behera B, Maiti T K, et al. Simple one-step synthesis of highly luminescent carbon dots from orange juice: application as excellent bio-imaging agents[J]. Chem Commun, 2012, 48(70): 8835-8837.

[19] Shen P, Gao J, Cong J, et al. Synthesis of cellulose-based carbon dots for bioimaging[J]. ChemistrySelect, 2016, 1: 1314-1317.

[20] Quang N K, Ha C T C. Low-cost synthesis of carbon nanodots from millets for bioimaging[J]. MRS Adv, 2019, 4(3-4): 249-254.

[21] Cao L, Wang X, Meziani M J, et al. Carbon dots for multiphoton bioimaging[J]. J Am Chem Soc, 2007, 129(37): 11318-11319.

[22] He L, Wang T, An J, et al. Carbon nanodots@zeolitic imidazolate framework-8 nanoparticles for simultaneous pH-responsive drug delivery and fluorescence imaging[J]. CrystEngComm, 2014, 16: 3259-3263.

[23] Liang Y, Zhang H, Zhang Y, et al. Simple hydrothermal preparation of carbon nanodots and their application in colorimetric and fluorimetric detection of mercury ions[J]. Anal Methods, 2015, 7: 7540-7547.

[24] Li H, Zhang Y, Wang L, et al. Nucleic acid detection using carbon nanoparticles as a fluorescent sensing platform[J]. Chem Commun, 2011, 47: 961-963.

[25] Li H, Chen L, Wu H, et al. Ionic liquid-functionalized fluorescent carbon nanodots and their applications in electrocatalysis, biosensing, and cell imaging[J]. Langmuir, 2014, 30(49): 15016-15021.

[26] Baker S N, Baker G A. Luminescent carbon nanodots: emergent nanolights[J]. Angew Chem Int Ed, 2010, 38: 6726-6744.

[27] Yang Y, Cui J, Zheng M, et al. One-step synthesis of amino-functionalized fluorescent carbon nanoparticles by hydrothermal carbonization of chitosan[J]. Chem Commun, 2012, 48: 380-382.

[28] Dong Y, Pang H, Yang H B, et al. Carbon-based dots co-doped with nitrogen and sulfur for high quantum yield and excitation-independent emission[J]. Angew Chem Int Ed, 2013, 52(30): 7800-7804.

[29] Jin X, Sun X, Chen G, et al. pH-sensitive carbon dots for the visualization of regulation of intracellular pH inside living pathogenic fungal cells[J]. Carbon, 2015, 81: 388-395.

[30] Li J Y, Liu Y, Shu Q W, et al. One-pot hydrothermal synthesis of carbon dots with efficient up- and down-converted photoluminescence for the sensitive detection of morin in a dual-readout assay[J]. Langmuir, 2017, 33(4): 1043-1050.

[31] Liu Y, Zhou Q, Yuan Y, et al. Hydrothermal synthesis of fluorescent carbon dots from sodium citrate and polyacrylamide and their highly selective detection of lead and pyrophosphate[J]. Carbon, 2017, 115: 550-560.

[32] Sharma V, Saini A K, Mobin S M. Multicolour fluorescent carbon nanoparticle probes for live cell imaging and dual palladium and mercury sensors[J]. J Mater Chem B, 2016, 4: 2466-2476.

[33] Titirici M M. Sustainable Carbon Materials from Hydrothermal Processes[M]. United Kingdom: John Wiley & Sons, 2013: 151-212.

[34] Lu W, Qin X, Liu S, et al. Economical, green synthesis of fluorescent carbon nanoparticles and their use as probes for sensitive and selective detection of mercury (II) ions[J]. Anal Chem, 2012, 84(12): 5351-5357.

[35] Du F, Zhang M, Li X, et al. Economical and green synthesis of bagasse-derived fluorescent carbon dots for biomedical applications[J]. Nanotechnology, 2014, 25(31): 315702-315711.

[36] Liu S, Tian J, Wang L, et al. Hydrothermal treatment of grass: A low-cost, green route to nitrogen-doped, carbon-rich, photoluminescent polymer nanodots as an effective fluorescent sensing platform for label-free detection of Cu (II) ions[J]. Adv Mater, 2012, 24(15): 2037-2041.

[37] Liu Y, Zhaoa Y, Zhang Y. One-step green synthesized fluorescent carbon nanodots from bamboo leaves for copper(II) ion detection[J]. Sens Actuators B, 2014, 196: 647-652.

[38] Qin X Y, Lu W B, Asiri A M, et al. Green, low-cost synthesis of photoluminescent carbon dots by hydrothermal treatment of willow bark and their application as an effective photocatalyst for fabricating Au nanoparticles–reduced[J]. Catal Sci Technol, 2013, 3: 1027-1035.

[39] Mota G S, Sartori C J, Ferreira J, et al. Cellular structure and chemical composition of cork from Plathymenia reticulata occurring in the Brazilian Cerrado[J]. Ind Crops Prod, 2016, 90: 65-75.

[40] Hill S, Galan M C. Fluorescent carbon dots from mono- and polysaccharides: Synthesis, properties and applications[J]. Beilstein J Org Chem, 2017, 13: 675-693.

[41] Nima A M, Amritha P, Lalan V, et al. Green synthesis of blue-fluorescent carbon nanospheres from the pith of tapioca (Manihot esculenta) stem for Fe (III) detection[J]. J Mater Sci: Mater Electron, 2020, 31(6): 21767-21778.

[42] Han X, Zhong S, Pan W, et al. A simple strategy for synthesizing highly luminescent carbon nanodots and application as effective down-shifting layers[J]. Nanotechnology, 2015, 26(6): 065402-065411.

[43] Zhu S, Song Y, Zhao X H, et al. The photoluminescence mechanism in carbon dots (graphene quantum dots, carbon nanodots, and polymer dots): Current state and future perspective[J]. Nano Res., 2015, 8(2): 355-381.

[44] Kwon W, Do S, Kim J H, et al. Control of photoluminescence of carbon nanodots via surface functionalization using parasubstituted anilines[J]. Sci Rep, 2015, 5: 12604-12613.

[45] Ding H, Li X H, Chen X B, et al. Surface states of carbon dots influences on luminescence[J]. J Appl Phys, 2020, 127: 231101-231121.

[46] Zhu S, Meng Q, Wang L, et al. Highly photoluminescent carbon dots for multicolor patterning, sensors, and bioimaging[J]. Angew Chem Int Ed, 2013, 52(14): 3953-3957.

[47] Zhu C, Zhai J, Dong S. Bifunctional fluorescent carbon nanodots: Green synthesis via soy milk and application as metal-free electrocatalysts for oxygen reduction[J]. Chem Commun, 2012, 48: 9367-9369.

[48] Vedamalai M, Periasamy A P, Wang C W, et al. Carbon nanodots prepared from o-phenylenediamine for sensing of Cu^{2+} ions in cells[J]. Nanoscale, 2014, 6: 13119-13125.

[49] Hsu P C, Chen P C, Ou C M, et al. Extremely high inhibition activity of photoluminescent carbon nanodots toward cancer cells[J]. J Mater Chem B, 2013, 1: 1774-1781.

[50] Jiang C, Wu H, Song X, et al. Presence of photoluminescent carbon dots in Nescafes original instant coffee: Applications to bioimaging [J]. Talanta. 2014, 127: 68-74.

[51] Li W, Yue Z, Wang C, et al. An absolutely green approach to fabricate carbon nanodots from soya bean grounds[J]. RSC Adv, 2013, 3: 20662-20665.

软木塞基碳量子点的水热合成及其生物相融荧光成像应用

Quang Ngo Khoa[1,*], Hieu Nguyen Ngoc[2,3], Bao Vo Van Quoc[4], Phuoc Vo Thi[1], Ngoc Le Xuan Diem[1], Doc Luong Quang[1], Tri Nguyen Minh[1], Son Le Vu Truong[5], Son Le Van Thanh[5], Ha Che Thi Cam[1]

(1. *University of Sciences*, *Hue University*, *77 Nguyen Hue*, *Hue*, *Vietnam*;
2. *Faculty of Environmental and Natural Sciences*, *Duy Tan University*, *Da Nang*, 550000, *Vietnam*;
3. *Institute for Research and Training in Medicine*, *Biology and Pharmacy*, *Duy Tan University*, *Da Nang*, 550000, *Vietnam*;
4. *University of Agriculture and Forestry*, *Hue University*, 102 *Phung Hung*, *Hue*, *Vietnam*;
5. *University of Science and Education*, *The University of Da Nang*, 459 *Ton Duc Thang*, *Lien Chieu*, *Da Nang*, *Vietnam*)

摘 要： 以废弃酒瓶软木塞为原料，采用低成本、简单的水热方法合成碳量子点。通过 TEM、FTIR、Raman、UV-Vis、PL 光谱对碳量子点的结构和光学性能进行分析表征。结果表明，碳量子点的平均直径为 6.2±2.7 nm，PL 激发谱和碳量子点表面的官能团有关。用硫酸奎宁作为参考，碳量子点的量子效率为 1.54%。将获得的碳量子点应用在骨髓间充质干细胞的细胞生物成像上，发现用碳量子点处理后，骨髓间充质干细胞分别在 320 ~ 380 nm、450 ~ 490 nm 和 450 ~ 490 nm 范围显示绿色、黄色和红色荧光，表明了碳量子点在荧光成像领域具有潜在的应用价值。

关键词： 碳点；水热合成；荧光；荧光图像；废酒瓶塞

文章编号： 1007-8827(2022)03-0595-08 **中图分类号：** TQ127.1^{+}1 **文献标识码：** A

基金项目：越南教育培训部项目（B2021-DHH-05）.

通讯作者：Quang Ngo Khoa. E-mail: nkquang@hueuni.edu.vn

本文的电子版全文由 Elsevier 出版社在 ScienceDirect 上出版（https://www.sciencedirect.com/journal/new-carbon-materials/）